

Potential of INSAT-3D Sounder Derived Total Precipitable Water Product for Weather Forecast

Shailesh Parihar^{*}, Ashim Kumar Mitra and ^aRajiv Bhatla

India Meteorological Department, New Delhi-110003

^a*Banaras Hindu University, Varanasi-221005*

*Email- shellsalpha@gmail.com

Abstract

The objectives of the INSAT-3D satellite are to enhance the meteorological observations and to monitor the Earth surface for weather forecasting and disaster warning. One of the weather monitoring capability in the INSAT-3D sounder is the estimation of water vapor in the atmosphere. The amount of the water vapor present in the atmospheric column is derived as the total precipitable water (TPW) product from the radiance measured by INSAT-3D sounder. The improvement in the estimation of TPW is carried out by applying the GSICS calibration corrections (Global Space-based Inter-Calibration System) to the radiances from Infra-Red (IR) channels of the sounder, which is done using IMDPS (INSAT Meteorological Data Processing System). The present study is based on TPW derived from INSAT-3D sounder, Radiosonde (RS) observations and National Oceanic and Atmospheric Administration (NOAA) N-18 and N-19 satellites. To assess retrieval performances of INSAT-3D sounder, RS observations carried out during May to September 2016 from 34 stations of India Meteorological Department (IMD) is considered for the validation. The analysis is performed on daily, monthly, and sub-divisional basis over the Indian region. The comparison of INSAT-3D TPW with RS TPW on daily and monthly basis shows that the root mean square error (RMSE) and correlation coefficients (CC) are ~8 mm and above 0.8, respectively. However, on sub-divisional and overall scale, the RMSE found to be in the range of 1 to 2 mm and CC was around 0.9 in comparison with RS and NOAA. The spatial distribution of INSAT-3D TPW with actual rainfall observation is also been investigated. In general, INSAT-3D TPW correspond well with rainfall observation however, heavy rainfall events occurs in the presence of high TPW values. In addition, utilizing the TPW from INSAT-3D and ground based Global Navigation Satellite System (GNSS) receiver network, the case studies of thunderstorm events shows good agreement during the mesoscale activity. The current TPW from

31 INSAT-3D satellite can be utilized operationally for weather monitoring and forecast purpose and
32 it can also offer substantial opportunities for improvement in nowcasting studies.

33 **Keywords:** INSAT-3D Sounder, Total Precipitable Water, rain fall.

34

35

1. INTRODUCTION

36 Water vapour is one of the most variable quantities in the troposphere, playing a crucial role in the
37 climate and weather. It regulates air temperature by absorbing thermal radiation both from the sun
38 and the Earth; it is directly proportional to the latent energy available for the generation of storms;
39 and it is the ultimate source of all forms of condensation and precipitation. Latent heat released
40 during cloud formation cloud dominate the structure of diabatic heating of the atmosphere
41 (Trenberth et al., 2005; Trenberth and Stepaniak, 2003a, b). The observations of Total Precipitable
42 Water (TPW) are essential for weather and climate modeling and prediction. The TPW may be
43 used for monitoring the mesoscale to synoptic scale convective activity, monsoonal activities, and
44 moisture gradients. Kuo et al., (1996) have shown the significant improvement in precipitation
45 forecasts when TPW is incorporated in the numerical weather prediction models. Utilizing the
46 TPW data, Yuan et al. (1993) showed ~8 mm increment in the tropical TPW resulting from
47 doubling of atmospheric CO₂. The water vapor varies in time and as well as in space (both
48 vertically and horizontally) and the gaps in the observations makes its use impossible for climate
49 and weather forecasting/nowcasting related studies (Trenberth and Olson 1988). This could be
50 possible with higher temporal and spatial resolution of accurate temperature and moisture profile
51 either from in-situ observations or remotely sensed data. Recently, The Sounder for Atmospheric
52 Profiles of Humidity in the Inter-tropical Regions (SAPHIR) on board Megha-Tropiques satellite
53 has made the RH profiles available in the tropical latitudes (Ratnam et al., 2013). SAPHIR has
54 good spatial coverage with limited temporal resolution.

55 The products, especially the retrievals of vertical profiles of temperature and humidity, from the
56 sounder of INSAT-3D satellite are important in weather monitoring and forecasting as well as in
57 the study of mesoscale weather phenomena. The higher ground resolution of 10 km and high
58 vertical resolution (about 1 km) along with hourly observations from INSAT-3D sounder provides
59 frequent information on the 3D structure of atmospheric temperature and humidity for the whole
60 Earth disk seen by the satellite (except in and below clouds). They could be used together with the

61 imagers, to produce high resolution cloud detection or water vapor features, to track rapidly
62 evolving phenomena. However, the INSAT-3D sounder observations of TPW are limited for sky
63 conditions (Ratnam et. al., 2016).

64 In the present study, the TPW derived from INSAT-3D sounder is statistically compared with
65 radiosonde observations and NOAA satellite data over the period May to September 2016. The
66 purpose of this comparison is to investigate the potential of operational hourly TPW product for
67 the monitoring of weather phenomenon over the Indian region. However, initial work using
68 INSAT-3D sounder data was carried out by Mitra et al. 2015, showing the comparison of INSAT-
69 3D data with RS observations from 10 stations of IMD (India Meteorological Department).
70 Utilizing the RS observations from 34 stations and data from ERA-Interim, NCEP re-analysis
71 and other satellites like AIRS, MLS, SAPHIR, Ratnam et al. 2016 showed the reasonable
72 agreement among these datasets. It is shown that there is a large difference between INSAT-3D
73 and other data sets; both in temperature and water vapour above 25 °N latitude; perhaps due
74 to difference in their geometries (Ratnam et al. 2016). In the present paper, we extend the work
75 with 34 RS stations and taking NOAA data on daily, monthly, sub divisional scale followed by
76 case studies with IMD installed network of GNSS TPW. Furthermore, the spatial distribution of
77 INSAT-3D TPW with actual rainfall observation has also been investigated.

78 **2. DATA BASE**

79 **2.1 INSAT-3D Sounder Scan processing strategy in IMD**

80 *2.1.1 INSAT-3D Sounder Specification*

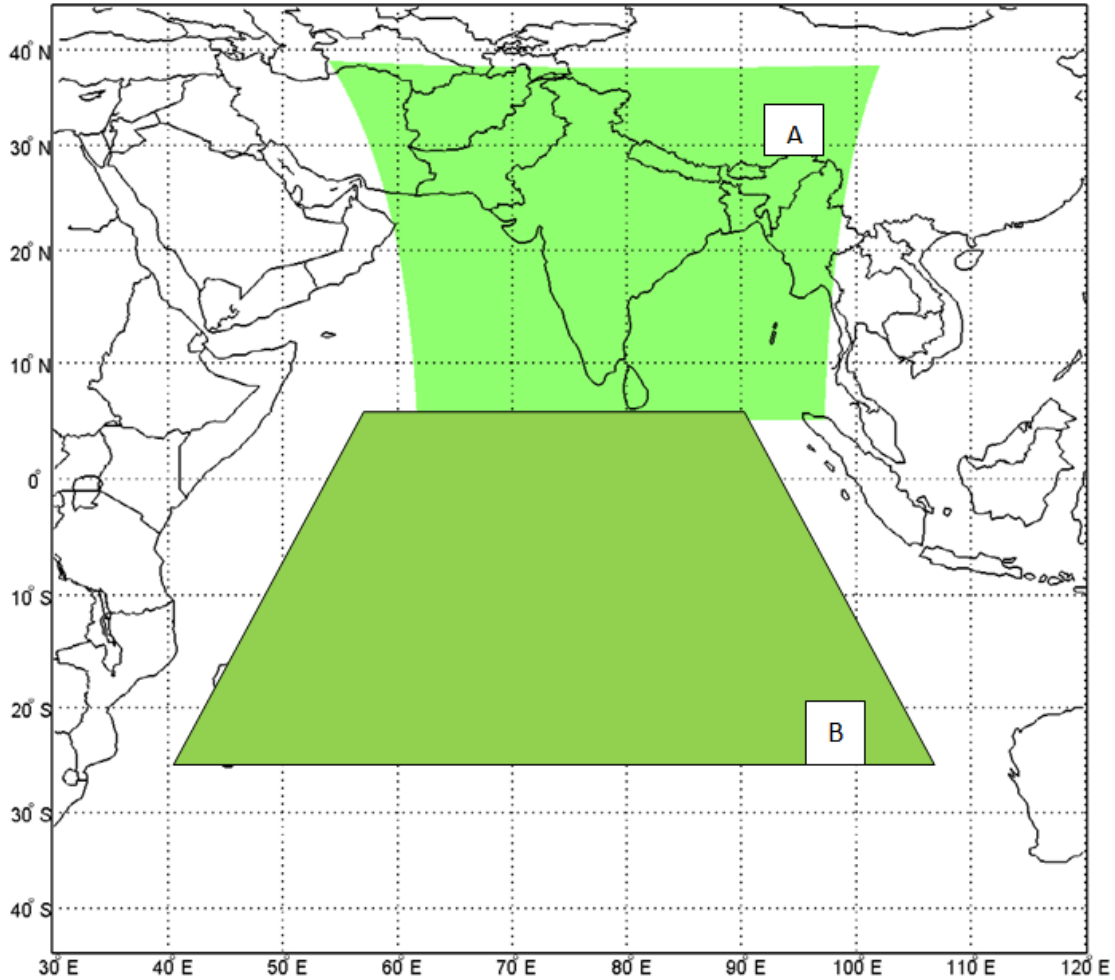
81 INSAT-3D is advance weather satellite with improved imaging system and atmospheric sounding.
82 The observations of INSAT-3D sounder are utilized to retrieve the vertical profile of the
83 atmosphere in terms of temperature and humidity. INSAT3D sounder has one visible spectral
84 channel and eighteen channels in shortwave infrared (SWIR), middle infrared (MIR) and long
85 wave infrared (LIR) regions. For all the channels, the ground resolution is 10×10 km. The further
86 detail of INSAT-3D sounder can be found elsewhere (Mitra et.al, 2015).

87 **Table 1Sounder Specification**

Channels (Spectral Range Microns)	Resolution
Visible (0.67)	10X10 Km
SWIR (3.67)	10X10 Km
MIR (6.38)	10X10 Km
LWIR (11.66)	10X10 Km

88 *2.1.2 INSAT-3D Sounder Scan processing Strategy*

89 INSAT-3D scans in the full frame mode which is $18^\circ \times 18^\circ$ North South (NS) covering the entire
90 Earth disc in about 25.7 minutes. Figure 1 shows the areas over Indian land mass (A) and over the
91 southern hemisphere (B) over which the sounder data is being processed by IMDPS
92 (Meteorological Data Processing System), New Delhi on an operational basis. While the Indian
93 land mass is scanned at every hour interval, it is 6 hour interval for the southern hemispheric area.
94 This is the simple scanning strategy kept in such a way that sounding over larger region (land +
95 ocean) will be available every hour. Sounder completes sounding in $10 \text{ km} \times 10 \text{ km}$ area in 0.1 s
96 and performs space look operation once every 2 minutes. Black body calibration is performed in
97 every 20 minutes or on command basis. INSAT-3D Sounder have a capability to scan in the steps
98 of 64×64 pixels. Scanning of a region covering 640×640 pixels that is roughly $6400 \text{ km} \times 6400$
99 km takes ~180 minutes. The benefit of this kind of scan strategy can be utilize for the studies of
100 initial convections, genesis of evolution of squall lines and their fine structures (Purdom 1996a).
101 The INSAT-3D sounder scan strategy can be used for nowcasting and NWP (Numerical Weather
102 Prediction) model assimilation over Indian region.



103

104

Figure 1. INSAT-3D Sounder scan processing strategy over land and ocean.

105

2.2 Radiosonde Observations (RS)

106

107

108

109

110

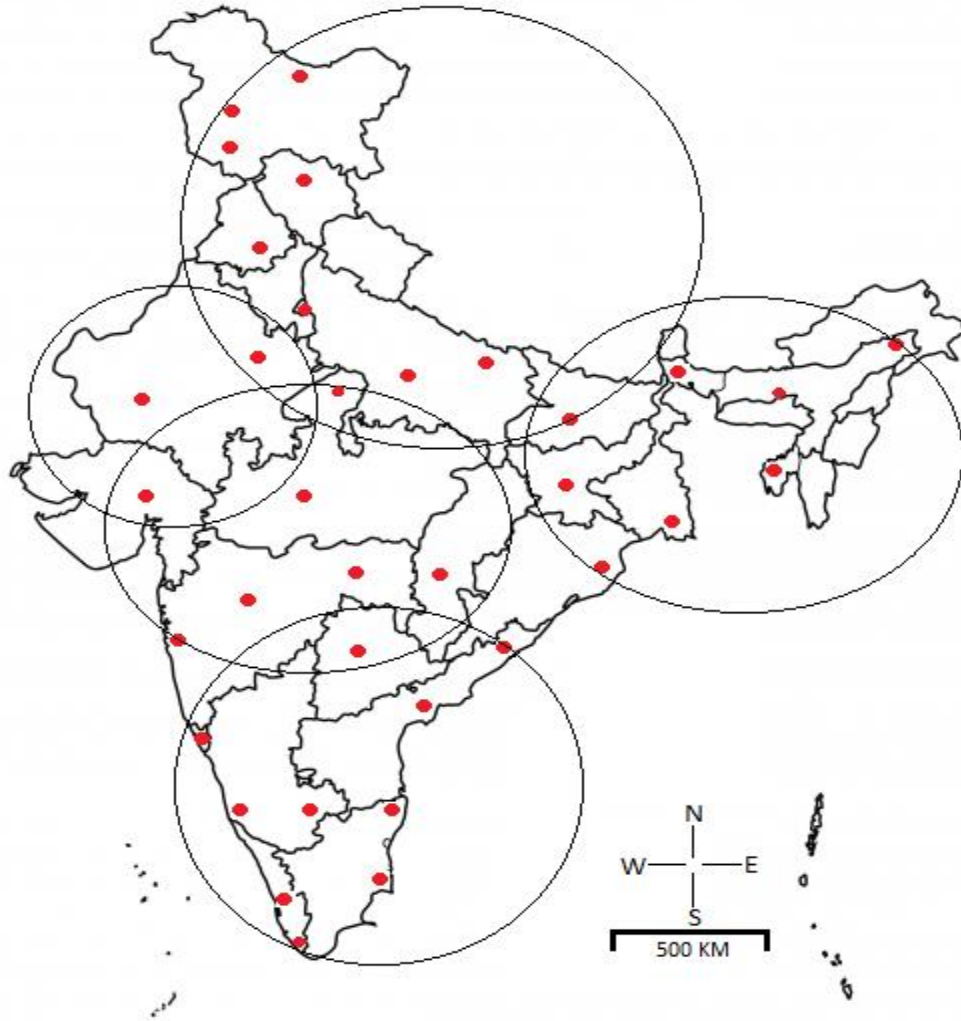
111

112

113

114

In IMD, upper air observations are made at 43 RS stations, 34 RS stations are being used and 62 Pilot Balloon observatories to provide pressure, temperature, humidity & wind at various levels in the atmosphere up to an altitude of 30-35 kms. Figure 2 shows the location (marked in red color) of 34 RS stations. Observations from these stations are utilised for the comparison with INSAT-3D TPW. The types of ground equipment used in RS observatories are (1) Radiosonde Ground equipment (ECIL/DIGITAL make) along with X band Win, (2) d finding Radars (EEC/MULTIMET) at 401 MHz and (3) IMS-1500 Radiotheodolite at 1680 MHz and SAMEER Radiotheodolite at 401 MHz. The performance of IMD's GPS radiosonde stations has been very well examined using ECMWF global data by Gajendra Kumar et al., (2011).



115

116

Figure 2. Radiosonde Stations of IMD over India

117

118 2.3 Global Navigation Satellite System (GNSS)

119 IMD is augmenting Integrated Network of Global Navigation Satellite System (GNSS) receivers
 120 from 5 to 30 for integrated precipitable water vapour (IPWV) measurements. The network is
 121 capable of using other GNSS Network data of research institutes in real time basis for enhancing
 122 data spatial density and processing. The equipment has advanced meteorological sensors to
 123 measure Temperature, Pressure, Humidity of the station and capable of working independently in
 124 all-weather condition with high temporal resolution. Though satellites don't often fail, if one fails

125 GNSS receivers can pick up signals from other satellites of the system.
126 (<http://gnss.imd.gov.in/TrimblePivotWeb/>)

127 **2.4 NOAA's satellite observation**

128 NOAA's (Oceanic and Atmospheric Administration) National Environmental Satellite Data and
129 Information Service works for the global community working on weather phenomenon. Advanced
130 Microwave Sounding Unit (AMSU) was aboard in the National's (NOAA) polar-orbiting satellites
131 N-18 and N-19. The TPW data for the study period was from www.nnvl.noaa.gov.

132 **2.5 GSICS based inter-calibration**

133 There is an on-board blackbody which is responsible for generation of calibration information
134 for all the IR channels in the sounder. In-orbit readings of blackbody
135 temperatures revealed a gradient among the sensor which led to inaccuracy in getting
136 the correct blackbody temperature. It was also observed that during satellite midnight, sun-rays
137 from behind the Earth enter directly into the sensor and hence lead to increase in blackbody
138 temperatures. This phenomenon leads to generation of incorrect calibration information. In order
139 to provide climate quality products and to improve the calibration coefficients,
140 GSICS (Global Space based Inter calibration System) based inter-calibration is used for INSAT-
141 3D. The GSICS aims to inter-calibrate a diverse range of satellite instruments, to produce
142 corrections ensuring consistency in satellite dataset. Allowing usage of calibration data, it produces
143 globally homogeneous products for environmental monitoring. In addition, GSICS develops
144 common methodologies to check the quality of sensors operated by various satellite agencies over
145 the worldwide. The post launch calibration strategy involves spectral response function of sensors,
146 sensor performances and inter-calibration of satellite sensor. And finally, recalibration of archived
147 data or products of sensors is carried out, if necessary. The channel wise GSICS coefficient are
148 found and applied in during the Radiometric Correction process.

149

150

3. METHODOLOGY

151 INSAT-3D retrieval algorithm under IMDPS at New Delhi, is designed for retrieving vertical
152 profiles of atmospheric temperature and moisture from clear sky infrared radiances measured over
153 different absorption bands. The observed radiance in various sounder channels are processed on

154 an hourly time scale. IMD, New Delhi has adapted sounder retrieval scheme from the operational
155 High resolution Infrared Radiation Sounder (HIRS) processing scheme and Geostationary
156 Operational Environmental Satellites (GOES) algorithms developed by Cooperative Institute for
157 Meteorological Satellite Studies (CIMSS), University of Wisconsin, USA (Ma et al., 1999 and Li
158 et al., 2000). In this scheme, physical and regression based retrievals are employed, which includes
159 spectral bands in and around the CO₂ and H₂O absorbing bands. In the scheme, computation of the
160 hybrid first guess atmospheric profiles is using a linear combination of regression retrieval and
161 NWP model forecast (Mitra et al., 2015). The methodology has followed by non-linear physical
162 retrieval procedure (Li et al., 2000; Ma et al., 1999) for the consistency with the sounder
163 observations. The Pressure layer Fast Algorithm for Atmospheric Transmittance (PFAAST)
164 radiative transfer model (Hanon et al., 1996) has been used for the forward computation of sounder
165 channel radiances along with the Jacobians. As mentioned before, GSICS corrections have been
166 incorporated in the INSAT-3D sounder radiances.

167 Mathematically, if $a(p)$ is the mixing ratio at the pressure level, p , then the precipitable water vapor
168 W , contained in a layer bounded by pressures p_1 and p_2 is given by

$$169 \quad \text{INSAT3D Precipitable Water Vapor} = \frac{1}{\rho g} \int_{p_1}^{p_2} a dp$$

170 Where ρ represents the density of water and g is the acceleration of gravity. Further details can be
171 found at <http://www.imd.gov.in/INSAT-3D/categouge>.

172 The each RS observation was paired with closest INSAT-3D TPW and patterned according to
173 criteria suggested in Fuelberg and Olson (1991). The collocation criteria for INSAT-3D retrievals
174 with RS and NOAA data are based on the following. (1) The absolute distance between the position
175 (latitude and longitude) of the RS and the INSAT-3D retrievals is 0.5° (50 Km) or smaller. This
176 will minimize the differences arising from horizontal gradients in water vapor or TPW. (2) The
177 temporal difference between two sets of data is around ± 120 minutes depending on retrievals and
178 location of the RS station. (3) The timing of INSAT-3D and RS observations was matched at 0000
179 and 1200 UTC.

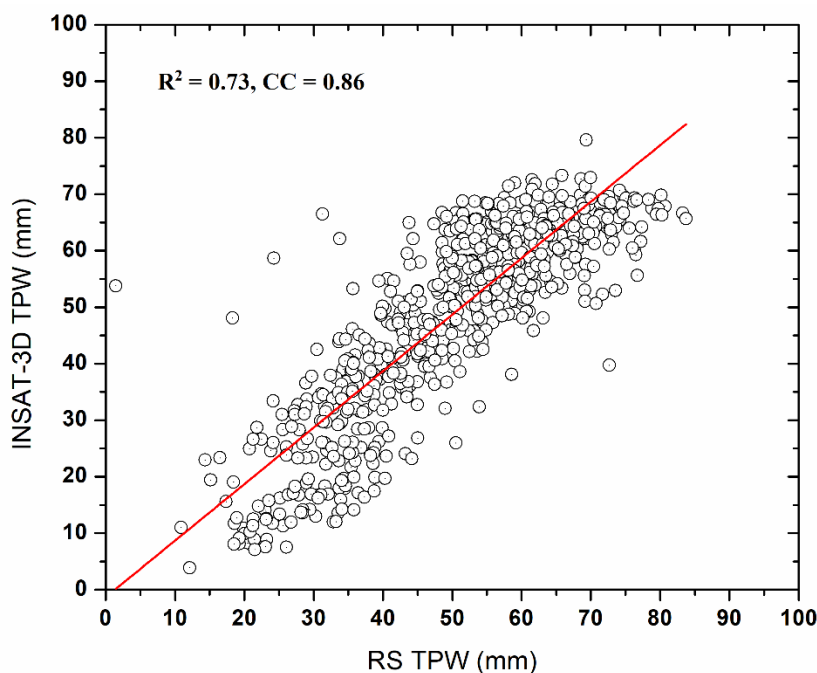
180

181

4. RESULTS AND DISCUSSIONS

182 **4.1 Comparison of INSAT-3D with RS and NOAA TPW at Daily, Monthly and**
183 **Sub divisional Scale**

184 INSAT-3D derived TPW is available at hourly interval over the Indian region. For validation
185 purposes of TPW and its usefulness in weather monitoring and forecast, it is desirable to compare
186 INSAT-3D TPW at different time scales with different sets of data. Thus, on a daily scale, we
187 compared the INSAT-3D TPW with all the collocated measurements of RS TPW. On monthly
188 scale, monthly averaged data on collocated points were used. For sub-division scale, five different
189 regions categorized according to meteorological subdivisions are, Northern India (NI), Eastern
190 India (EI), Central India (CI), Western India (WI) and Peninsular India (PS) (figure 2).



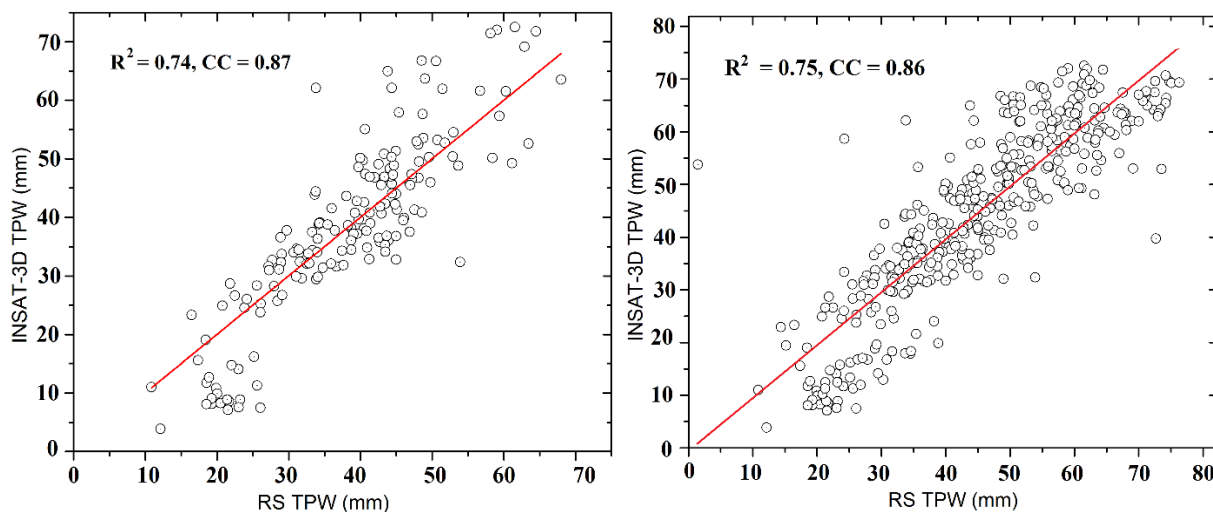
191
192 **Figure 3. INSAT-3D sounder TPW with RS for Day-wise from May to September 2016**

193 Figure 3 shows the comparison of INSAT-3D TPW and RS TPW on daily scale during May-
194 September 2016. On day to day basis, INSAT-3D TPW agrees well with RS TPW. The consistent
195 and better correlation has seen above 40 mm of TPW values, whereas for less than 40 mm TPW
196 values, INSAT-3D underestimates slightly. This may be attributed to seasonal variation,
197 orographic of the region and different climatic zone over India. The overall correlation on daily
198 scale was found to be 0.86. In the previous study, Mitra et al. (2015) have reported 0.73 correlations
199 using 10 IMD stations.

200 Figure 4 shows the comparison of INSAT-3D TPW and RS TPW on Monthly scale during May-
201 September 2016. The correlation coefficients are in the range of 0.78-0.87. It can be noticed that
202 during monsoon period, specially in the month of June, July and August, when heavy rainfall
203 (above 64.5 mm) occurs, INSAT-3D TPW shows well agreement with RS TPW. Mostly INSAT-
204 3D TPW is higher when rainfall occurrence is higher above 40 mm.

205 The statistics corresponding to this comparison is shown in table 2. INSAT-3D coefficients of
206 variation are high as compared with RS, which indicates the higher variability in total precipitable
207 water. The coefficient of variation is lower for the months July to September, 2016. The coefficient
208 of skewness found negative between INSAT-3D and RS measurement, which indicates mean is
209 less than the mode of the data. The correlation coefficient show good agreement with RMSE for
210 June to September, 2016 except in the month of July. The student's t-test calculated for
211 significance of computed parameter. The student's t-test shows the statistical significance of linear
212 relationship among the data, i.e. INSAT-3D TPW and RS TPW.

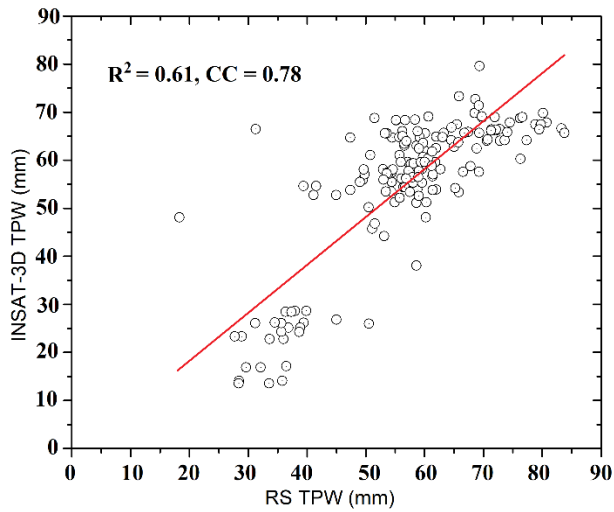
213



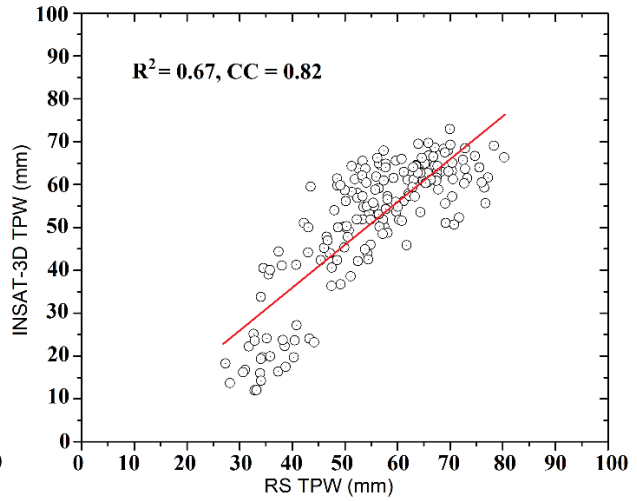
214

215

(a) (b)



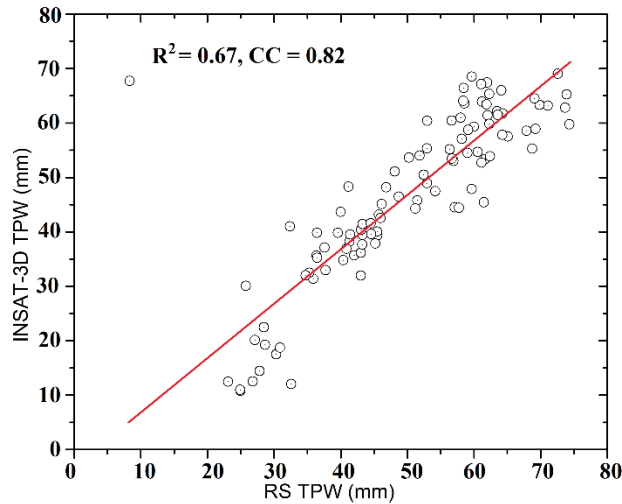
216



217

(c)

(d)



218

(e)

219

220 **Figure 4. INSAT-3D sounder TPW with RS for (a) May (b) June (c) July (d) August and (e)**
 221 **September 2016**

222

223 **Table 2. Statistics and correlation between total precipitable water measured by INSAT-3D**
 224 **and RS**

Month	INSA T-3D	RS	INSA T-3D	RS	IN SA T- 3D	RS	IN SA T- 3D	RS	CC	R MS E(t-test
-------	--------------	----	--------------	----	----------------------	----	----------------------	----	----	---------------	--------

	Arithmetic Mean (mm)		Standard Deviation		Coefficient of Variation		Coefficient of Skewness		0.87	m m)	
May	39.36	39.87	15.40	12.51	0.39	0.31	-0.21	-0.10	7.69	0.359931	
Jun	49.75	52.66	16.44	14.16	0.33	0.26	-0.87	-0.57	8.50	0.049282	
July	54.87	60.44	14.59	12.53	0.26	0.20	-1.45	-0.61	9.31	0.000012	
Aug	52.09	57.33	14.71	11.97	0.28	0.20	-1.24	-0.49	8.73	0.000022	
Sep	49.00	54.30	14.14	13.69	0.28	0.25	-1.01	-0.31	8.79	0.000213	

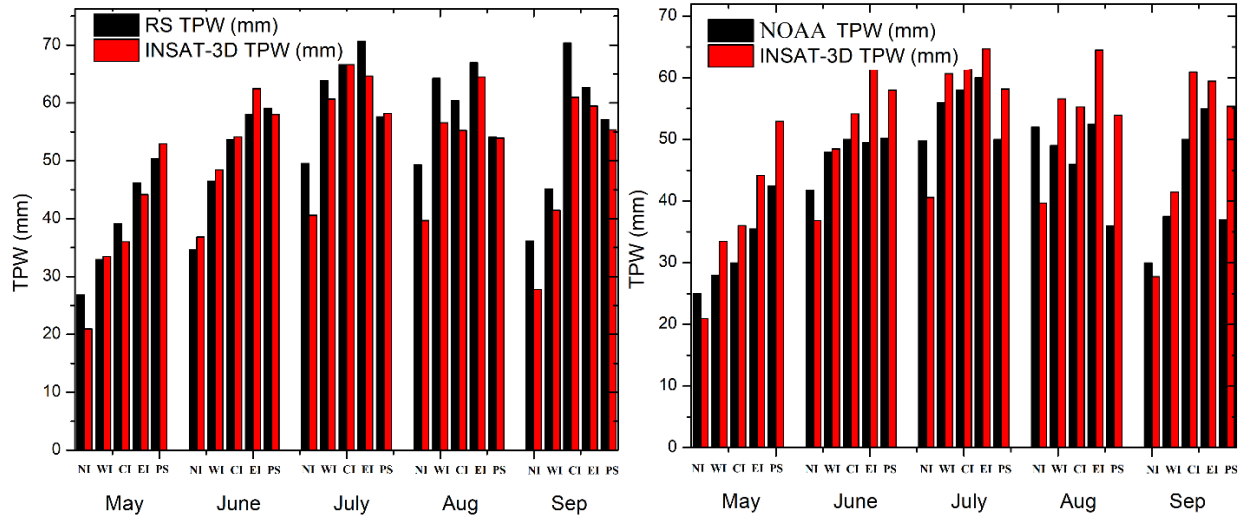
225

226 Figure 5 shows the comparison of INSAT-3D TPW with RS TPW and NOAA TPW on sub
 227 divisional scale during May to September 2016. It can be clearly seen from the figures that INSAT-
 228 3D TPW is underestimating whereas it is over estimating the NOAA TPW for the entire region
 229 during the monsoon period.

230 A good correlation is observed for the region, CI and PS as compared to EI and NI regions.
 231 However, opposite trend were found while comparing INSAT-3D TPW with NOAA TPW.
 232 INSAT-3D TPW is always higher over NOAA data. One of the possible reasons is that INSAT-
 233 3D sounder derived TPW were calculated from the radiances sampled every hour while NOAA
 234 TPW were based on only two satellite passes with equator crossing times of 0230 and 1430 local
 235 time. Therefore, the sampling frequency of the radiometer is much higher in a geostationary
 236 satellite than polar satellite. In general, sub-divisional comparison reveals that the INSAT-3D
 237 TPW agrees well RS and NOAA TPW below 23°N whereas the difference is higher above 23°N.

238 The table 3 shows the statistics for the comparison of TPWs from INSAT-3D, RS and NOAA at
 239 the subdivisions in India. INSAT-3D coefficients of variation are similar to that of RS, but in case
 240 of NOAA it is higher with respect to INSAT-3D and RS. The coefficient of skewness values found
 241 negative for INSAT-3D, RS and NOAA measurement. The correlation coefficients show good
 242 agreement between INSAT-3D and NOAA (0.96) as well as between INSAT-3D and RS (0.87)
 243 during June to September, 2016.

244



245
246 **Figure 5. Subdivision wise NI, WI, CI, WI & PS from May to September 2016 between**
247 **INSAT-3D and RS (left), NOAA (right)**

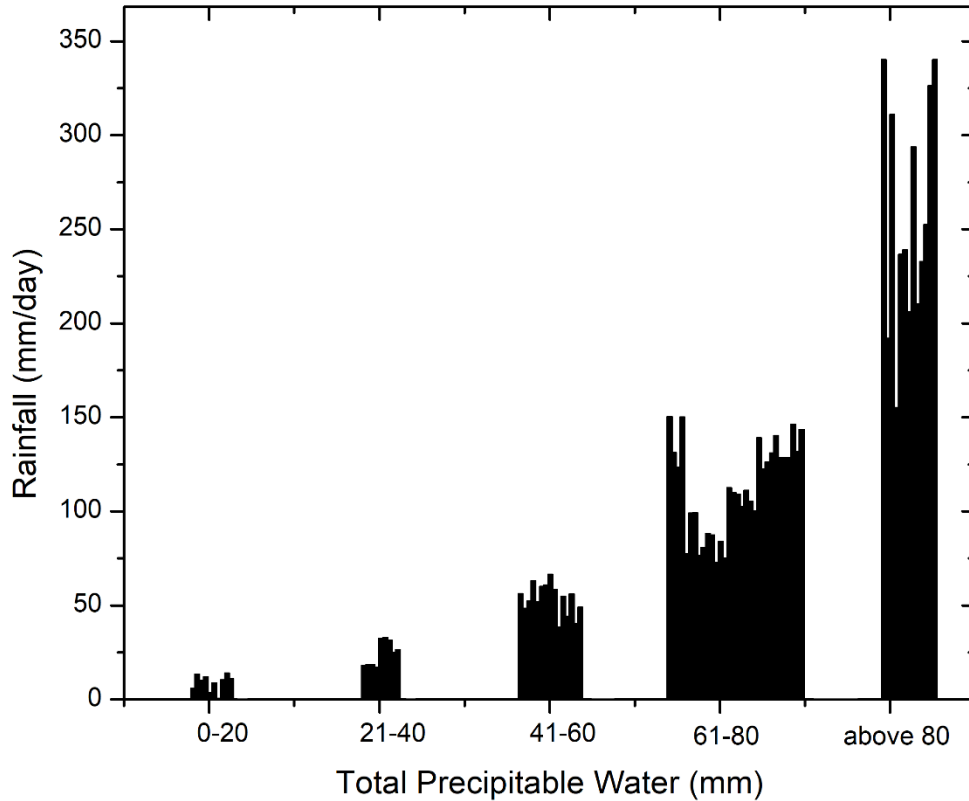
248 **Table 3. Statistics for total precipitable water measured by INSAT-3D, RS and NOAA**
249 **sub divisional regions of India**

Sub div.	Sensors	Arithetic Mean	SD	Coefficient of Variation	Coefficient of Skewness	NOAA vs INSAT-3D			INSAT-3D vs RS		
						BIAS	RMSE	CC	BIAS	RMS E	CC
NI	NOAA	39.71	11.91	0.30	-0.29	1.3	1.09	0.97	1.22	1.15	0.87
	INSAT-3D	33.16	8.51	0.25	-0.84						
	RS	39.28	9.91	0.25	0.005						
WI	NOAA	43.7	10.98	0.25	-0.63	-0.88	0.88	0.97	0.47	0.77	0.97
	INSAT-3D	48.13	11.04	0.22	-0.26						
	RS	50.52	13.42	0.26	-0.12						
CI	NOAA	46.8	10.35	0.22	-1.22	-1.56	1.23	0.97	0.79	0.83	0.96
	INSAT-3D	54.61	11.51	0.21	-1.20						
	RS	58.58	12.83	0.21	-0.90						
EI	NOAA	50.5	9.22	0.18	-1.28	-1.71	1.27	0.91	0.37	0.83	0.91
	INSAT-3D	59.05	8.58	0.14	-1.92						
	RS	60.92	9.47	0.15	-1.00						
PS	NOAA	43.14	6.81	0.15	0.10	-2.5	1.55	0.77	-	0.002	0.45
	INSAT-3D	55.68	2.36	0.04	0.05						
	RS	55.66	3.44	0.06	-1.00						

250

251 **4.2 Comparison of spatially analyzed INSAT-3D TPW with Actual Rainfall** 252 **Observation**

253 Figure 6, shows the comparison of rainfall and TPW for different INSAT-3D TPW values during
254 June to September 2016. This figure is constructed from the daily rainfall observation between 0
255 to 140 mm occurring over the stations and collocated mean INSAT-3D TPW values between 0 to
256 90 mm. It can be seen from the figure 6, that higher rainfall amount is accounted with higher
257 INSAT-3D TPW values. However, atmospheric constituents and synoptic scale of monsoon
258 conditions are an important factor when considering the occurrence of rainfall and satellite derived
259 TPW. It is well demonstrated from the figure 6, that the heavy and heavy to very heavy rainfall
260 are corresponding to the higher TPW values (60-80 mm and above 80mm). This can be obviously
261 related to the fact that the heavy rainfall occurs in the presence of higher TPW values (Wu et al,
262 2003). However, for the light to moderate rainfall amount (less than 40 mm) INSAT-3D TPW is
263 comparable. The moisture convergence, advection of moisture over geographical locations of the
264 subdivisions occasionally receive heavy to very heavy rainfall due to synoptic scale monsoon
265 circulations or due to its orography during the summer monsoon season. The areas having high
266 orographic region like north eastern parts, Jammu-Kashmir and parts of the Western Ghats (in the
267 west coast of India), have less evaporation and high rainfall as the moisture laden air mass is
268 transported over the regions. Similarly, it is also observed that the rainfall is overestimated in the
269 dry conditions because the falling raindrop evaporates before coming to the surface in dry
270 conditions resulting in the overestimation of rainfall.



271

272

Figure 6. Overall comparison of rainfall with INSAT-3D TPW

273

274 **4.3 Case studies of INSAT-3D TPW with ground base GNSS TPW**

275 In these case studies, hourly INSAT-3D sounder derived TPW, and GNSS TPW were analyzed
 276 for a thunderstorm events occurred in Pune, lat/lon 18.52°/73.85° on 03.06.2017 at 1200 UTC,
 277 Kochi, lat/lon 9.93°/76.26° on 06.06.2017 at 0600 UTC and Dibrugarh lat/lon 27.47°/94.91° on
 278 09.06.2017 at 0000 UTC. The advantage of GNSS is having access to multiple satellites,
 279 redundancy and availability at all times.

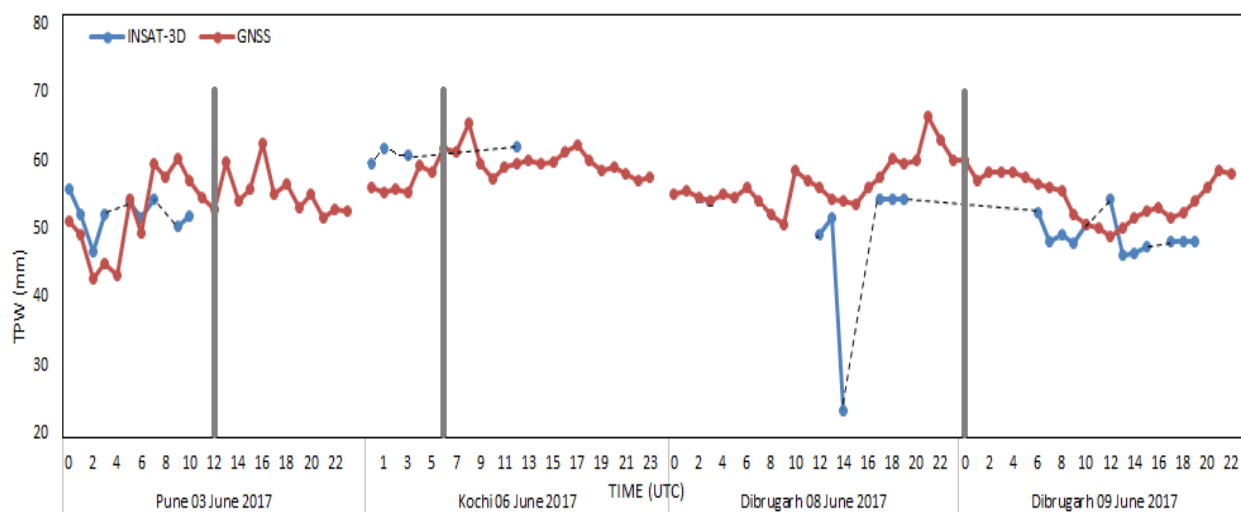
280 Figure 7 shows the hourly comparison between TPW derived from INSAT and GNSS during
 281 thunderstorm events. The grey bar shows the time of occurrence (i.e., 1200 UTC) of thunderstorm
 282 over Pune city. It was observed from the satellite imageries (not shown here) that initial convection
 283 development starts at 0600 UTC with multiple significant convections. It can be seen from the
 284 figure-7 that the INSAT-3D TPW is showing the higher TPW values around 53 mm in comparison
 285 with GNSS TPW of 54 mm at 0600 UTC. The higher TPW of INSAT-3D continues up to 1100
 286 UTC which is in agreement with GNSS TPW. The thunderstorm was reported at 1200 UTC. Since

287 INSAT-3D retrieval cannot be made over cloudy region, the TPW observation was not available
288 after 1200 UTC.

289 In case of the event at Kochi city, the grey bar shows the time of occurrence at 0600 UTC of
290 thunderstorm. It was observed from the satellite imageries that initial convection development
291 starts at 0100 UTC. INSAT-3D TPW is showing the higher TPW values around 58 mm in
292 comparison with GNSS TPW of 51 mm at 0100 UTC. The TPW observation was not available
293 after the 0300 UTC due to cloudy conditions. The higher TPW of INSAT-3D continues up to 0300
294 UTC in agreement with GNSS TPW and thunderstorm was observed at 0600 UTC.

295 At 0000 UTC of thunderstorm over Dibrugarh city was reported. The initial convection
296 development started at 1800 UTC with values around 53 mm in comparison with GNSS TPW of
297 58 mm at 1800 UTC. The higher TPW of INSAT-3D continues up to 2000 UTC which is in
298 agreement with GNSS TPW. The thunderstorm was reported at 0000 UTC on 09.06.2017.

299 This shows that during the thunderstorm events, INSAT-3D derived TPW compares well with
300 GNSS TPW, showing the potential of INSAT-3D derived TPW for the studies on thunderstorm
301 events. Along with other meteorological parameters (e.g., CAPE; convective available potential
302 energy), higher TPW observed during thunderstorm events can be utilized for studying such
303 events. However, the above case studies confirms the usefulness of INSAT-3D derived TPW prior
304 to the event and it can be considered as one of the precursors for mesoscale activity.



305
306 **Figure 7. A thunderstorm weather event in Pune on 03.06.2017, Kochi on 06.06.2017 and**
307 **Dibrugarh on 08-09.06.2017**

308

309

310

5. CONCLUSION

311 In the present study, INSAT-3D sounder derived TPW and corresponding TPW from radiosonde
312 (RS) observations, National Oceanic and Atmospheric Administration (NOAA) N-18 and N-19
313 and Global Navigation Satellite System (GNSS) receiver network have used to assess retrieval
314 performances of TPW product of INSAT-3D sounder. The comparison carried out at daily,
315 monthly and sub-divisional scale covering the entire South Asian monsoon season with different
316 geographical region of the Indian sub-continent. The INSAT-3D derived TPW are in good
317 agreement (correlation coefficients ~ 0.8) with the TPW derived from in situ measurement (RS)
318 and other satellites. It is to be noted that the INSAT-3D TPW on monthly scale show very good
319 agreement with the sub divisional scale rainfall observations; indicating the reliability to use the
320 TPW product for the advancement of monsoonal pattern over Indian region. The improvement
321 observed in the current INSAT-3D sounder products-TPW is mainly attributed to the GSICS bias
322 corrections applied to the sounder radiances at IMDPS by SAC/ISRO. The advantages of INSAT-
323 3D TPW are the availability of the real-time data over the Indian region due to higher spatial and
324 temporal resolution as compared to polar orbiting satellites. The quality of TPW product of
325 INSAT-3D shows the potential for its usefulness in weather monitoring, forecast purpose and also
326 for the improvement in nowcasting. In addition, TPW can also be utilized for the study
327 of mesoscale activity like thunderstorm.

328

329

ACKNOWLEDGMENTS

330 Authors are very much grateful and rendered by Director General of Meteorology Dr. K. J.
331 Ramesh, and given valuable suggestions. We specially thank C.M Kistawal and P. Thapliyal for
332 the improvement of INSAT-3D sounder retrievals specially the applying of the GSICS corrections
333 at IMDPS for the improvement sounder retrievals and their technical inputs. First authors also
334 thankful to NOAA for providing us required data and GSICS members for providing technical
335 support.

REFERENCES

- 337 Ackerman, S. A. and G. L. Stephens, 1987: The absorption of solar radiation by cloud droplets:
338 An application of anomalous diffraction theory. *J. Atmos. Sci.*, 44, 1574-1588.
- 339 Gajendra Kumar, Ranju Madan, K.C. Sai Krishnan & P. K. Jain, 2011, Technical and operational
340 characteristics of GPS radiosounding system in upper air network, *MAUSAM*, 62, 3, pg 403-416
- 341 Hannon, S., Strow, L. L. and McMillan, W. W., 1996, “Atmospheric Infrared fast transmittance
342 models: A comparison of two approaches”, *Proc. SPIE – Int. Soc. Opt. Eng.*, 2830, 94-105.
- 343 Kuo, Y. H., Zou, X. and Guo, Y. R., 1996, “Variational assimilation of precipitable water
344 using a non-hydrostatic mesoscale adjoint model”, *Mon. Wea. Rev.*, 124, 122-147.
- 345 Li, J. and Huang, H. L.: Retrieval of atmospheric profiles from satellite sounder measurements by
346 use of the discrepancy principle, *Appl. Optics*, 38, 916–923, 1999.
- 347 Li, J., Wolf, W. W., Menzel, W. P., Zhang, W., Huang, H. L., and Achtor, T. H.: Global soundings
348 of the atmosphere from ATOVS measurements: The algorithm and validation, *J. Appl. Meteorol.*,
349 39, 1248–1268, 2000.
- 350 Ma, X. L., Schmit, T., and Smith, W.: A non-linear physical retrieval algorithm – Its application to
351 the GOES-8/9 sounder, *J. Appl. Meteor.*, 38, 501–503, 1999.
- 352 Mitra, A., Bhan, S., Sharma, A., Kaushik, N., Parihar, S., Mahandru, R., and Kundu, P. K.: INSAT-
353 3D vertical profile retrievals at IMDPS, New Delhi, *Mausam*, 66, 687–694, 2015.
- 354 Ratnam, M. V., Basha, G., Murthy, B. V. Krishna, Jayaraman, A.: Relative humidity distribution
355 from SAPHIR experiment on board Megha-Tropiques satellite mission: Comparison with global
356 radiosonde and other satellite and reanalysis data sets, 118, 1-9, 2013.
- 357 Ratnam, M. V., Kumar, A. H., Jayaraman, A.: Validation of INSAT-3D Sounder data with in-situ
358 measurements and other similar satellite observations over India, *J. Atmospheric measurement*
359 *techniques*, 9, 5735–5745, 2016.
- 360 Susskind, J., Barnett, C., Blaisdell, J., Iredell, L., Keita, F., Kouvaris, L., Molnar, G., and Chahine,
361 M.: Accuracy of geophysical parameters derived from Atmospheric Infrared Sounder/Advanced
362 Microwave Sounding Unit as a function of fractional cloud cover, *J. Geophys. Res.*, 111, D09S17,
363 doi: 10.1029/2005JD006272, 2006.

364 Trenberth, K. E. and Stepaniak, D. P.: Seamless poleward atmospheric energy transports and
365 implications for the Hadley circulation, *J. Climate*, 16, 3706–3722, 2003a.

366 Trenberth, K. E. and Stepaniak, D. K.: Covariability of components of poleward atmospheric
367 energy transports on seasonal and inter annual timescales, *J. Climate*, 16, 3691–3705, 2003b.

368

369 Trenberth, K. E., Fasullo, J., and Smith, L.: Trends and variability in column-integrated
370 atmospheric water vapor, *Clim. Dyn.*, 24, 741–758, 2005.

371 Wu, P., J.-I. Hamada, S. Mori, Y. I. Tauhid, M. D. Yamanaka, and F. Kimura, 2003: Diurnal
372 variation of precipitable water over a mountainous area of Sumatra Island. *J. Appl. Meteorol.*,
373 42, 1107-1115

374 Yuan, L., Anthes, R., Ware, R., Rocken, C., Bonner, W., Bevis, M. and Businger, S., 1993,
375 “Sensing climate change using the global positioning systems”, *J. Geophys. Res.*, 98, 14,925-
376 14,937.